Journal of Chromatography, 444 (1988) 303–324
Elsevier Science Publishers B.V., Amsterdam — Printed in The Netherlands

CHROMSYMP. 1333

PREPARATIVE SEPARATION OF PEPTIDE AND PROTEIN SAMPLES BY HIGH-PERFORMANCE LIQUID CHROMATOGRAPHY WITH GRADIENT ELUTION

I. THE CRAIG MODEL AS A BASIS FOR COMPUTER SIMULATIONS

L. R. SNYDER*
LC Resources Inc., 26 Silverwood Court, Orinda, CA 94563 (U.S.A.)
and
G. B. COX and P. E. ANTLE
Medical Products Department, E. I. Du Pont de Nemours, Wilmington, DE 19898 (U.S.A.)

SUMMARY

The Craig model (assuming a Langmuir isotherm) has been used by us previously to successfully simulate isocratic high-performance liquid chromatographic (HPLC) separation in a mass-overload mode. Here we have extended this approach to the case of gradient elution for large samples. These simulations support our earlier conclusion that so-called "corresponding" isocratic and gradient separations provide similar sample resolution when the sample size is the same. "Corresponding" separations refer to the case where isocratic retention k' is equal to average gradient retention $\bar{k}$, and where other conditions (column, flow-rate, etc.) are the same. Craig simulations reported here also provide further insight into the factors that affect preparative HPLC separations under mass-overload conditions.

INTRODUCTION

High-performance liquid chromatography (HPLC) is being used increasingly for the separation and purification of peptides and proteins[1,2], usually in a gradient elution mode. These separations are now carried out on a pilot plant or process scale, involving sample sizes of grams to kilograms. It is therefore becoming increasingly important to have a good understanding of how separation varies with experimental conditions, including sample mass. Ideally, we would like to be able to predict separation quantitatively as a function of different separation variables. Even more important is the development of general relationships between preparative separation and various experimental conditions including sample size; these relationships should allow a better understanding by practical workers of how to optimize a particular separation.

Several groups have reported results for the mass-overloaded separation of protein samples as a function of sample size, column type (particle size, pore-diameter,

0021-9673/88/$03.50 © 1988 Elsevier Science Publishers B.V.

etc.) and other variables[3–10]. While this work includes fundamental studies that have been correlated with theoretical models[7,9], the remaining studies are more empirical and do not encourage quantitative generalizations. We have approached this problem from a different direction, starting with simple systems that allow the construction of quantitative and detailed models that describe the separation process. Earlier work from our group has resulted in the development of general theories for (a) the analytical-scale separation of large biomolecules by HPLC[11] and (b) the preparative separaton of small molecules[12–16]. In the present series of papers, we hope to extend this treatment to include the case of large samples of peptides and proteins separated by gradient elution.

As a first step, we consider in this paper the mass-overloaded separation of small molecules by gradient elution. We have previously treated this subject in preliminary fashion[17]. There it was shown that the same resolution results from "corresponding" isocratic and gradient elution systems, when sample size and other conditions are comparable. Since it is now possible to predict isocratic separation in an overload mode by means of our model[16], it follows that gradient separations can be treated in terms of equivalent ("corresponding") isocratic separations. One aim of the present paper is to further confirm the conclusions reached in ref. 17. Additional questions also arise for the case of protein samples and for severely overloaded runs (which are more often practical in separations of protein samples). For these and other reasons, we have expanded our treatment of ref. 17 as described in the present paper. The following discussion is directed primarily at reversed-phase separation, but our general conclusions should apply qualitatively to other HPLC procedures as well.

THEORY

Craig-distribution model for gradient elution

The Craig-distribution model has been used previously as an approximation to various chromatographic processes, *e.g.*, isocratic chromatography with small samples[18], the generation of artifactual peaks as a result of competitive or cooperative sorption effects[19], and (by us) the simulation of mass-overloaded isocratic HPLC[12,14]. Its extension here to the case of mass-overloaded gradient elution is similar to that described in ref. 12.

We assume a Langmuir isotherm, which —with certain additional approximations (see ref. 12)— yields the following relationships

$$(w_{xs}n_c)/w_s = k_0C_x/(\psi + k_0C_x) \quad (1)$$

$$w_x/w_s = [(w_{xs}n_c)/w_s] + C_x/\psi \quad (2)$$

$$R = C_x/(w_x\psi) \quad (3)$$

Here w_{xs} is the mass of solute X in the stationary phase of a Craig stage, n_c is the number of Craig stages in the column, w_s is the saturation uptake of X by the stationary phase for the entire column, k_0 is the value of the capacity factor k' for a small sample (no mass overload), C_x is the concentration of X in the mobile phase, and ψ is the phase ratio (w_s/V_m, where V_m is the volume of mobile phase in one stage).

R is not definable by an explicit function of k_0 and w_x, thus requiring a numerical procedure for calculating R for each stage after each mobile phase transfer.

Previously[12], we used a polynomial in w_x for predefined values of k_0. This approach is not practical for gradient elution, because a very large number of different k_0 values are involved in each simulated run. An iterative solution was considered to be too time-consuming to allow its use with large numbers of Craig stages (n_c). As an alternative, we were able to construct an empirical algorithm which has been found accurate within $\pm 2\%$ (average) in R over wide ranges in k_0 and w_x (see Appendix I).

Conditions for a gradient run are summarized by values of k_{0g}, b and t_0. The quantity k_{0g} refers to the value of k_0 for the solute at the beginning of the gradient, t_0 is the column dead-time, and b is a gradient-steepness parameter defined by[20]

$$\log k_i = \log k_{0g} - b(t/t_0) \tag{4}$$

Here k_i refers to the value of k_0 at the column inlet at time t after the start of the gradient. Eqn. 4 defines a so-called linear-solvent-strength gradient[20], which is assumed in the present treatment. In our Craig model for gradient elution under mass overload conditions, the value of k_0 (k_i) for the first Craig stage was changed in accordance with eqn. 4, and transferred successively (with the associated mobile phase volume) to later stages as in ref. 12.

Bandwidth vs. solute mass in isocratic separation (Craig model)

In the following treatment it is useful to compare bandwidths from corresponding isocratic and gradient separations, as obtained from the Craig model. Knox and Pyper have shown (ref. 21 with modifications of ref. 16) that bandwidth in mass-overloaded separations can be expressed as

$$N/N_0 = 1/[1 + (p/4)\, w_{xn}] \tag{5}$$

where N is the plate number for a band of interest, N_0 is the value of N for a small sample, p is an adjustable parameter assumed equal to 1 by Knox and Pyper*, and w_{xn} is given by

$$w_{xn} = [k_0/(1 + k_0)]^2\, N_0\, (w_x/w_s) \tag{6}$$

Finally, bandwidth W is equal to

$$W = 4\, t_0\, (1 + k_0)\, N^{-1/2} \tag{7}$$

Eqn. 5 correlates well with experimental data when a value of $p = 1.5$ is assumed[16]. Comparisons of bandwidths from Craig simulations with experimental values show a 2.4-fold discrepancy in corresponding values of w_s[13,15], suggesting that p should equal $(1.5/2.4) = 5/8$ for the application of eqn. 5 to bandwidths from Craig simulations. This hypothesis is tested in Fig. 1, where experimental values of (N/N_0) from Craig simulation[12] are plotted *vs.* w_{xn}. The solid curve predicted by eqn. 5 with $p = 5/8$ fits

* Poppe and Kraak find $p = 0.9$ in their definitive early paper on mass-overload effects in HPLC (see eqn. 15 of ref. 22).

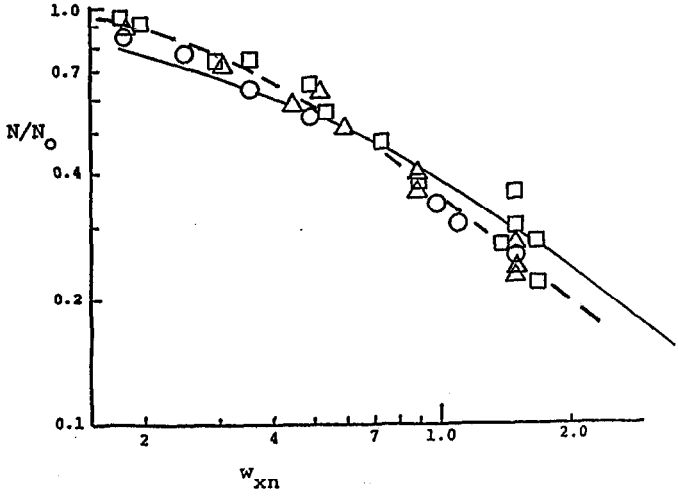

Fig. 1. Values of (N/N_0) from Craig simulation[12] *vs.* loading function w_{xn}. (□) $n_c = 200$; (○) $n_c = 600$; (△) $n_c = 1000$; (——) eqn. 5, $p = 5/8$; (– – –) best-fit curve.

these data reasonably well. At this time, it is not known why this discrepancy (different values of p) exists for experimental *vs.* Craig-simulation bandwidths.

When the sample size w_x is large, overloaded bands will assume a right-triangular shape[16], and bandwidth can be approximated by

$$W = t_0 (k_0 - k') \tag{7a}$$

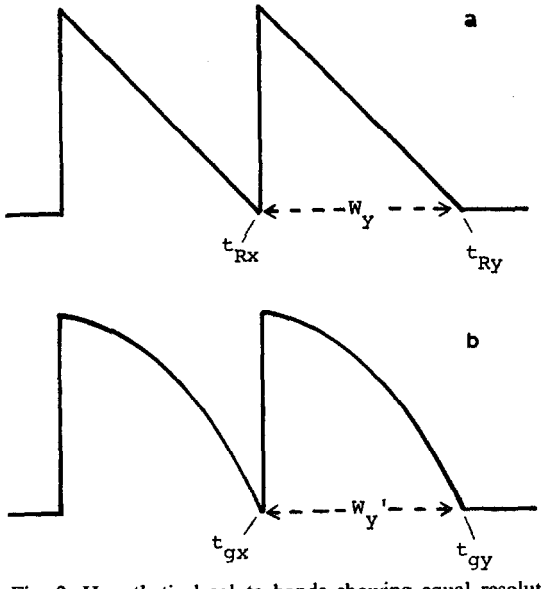

Fig. 2. Hypothetical solute bands showing equal resolution in (a) isocratic and (b) gradient elution. Definition of small-sample retention times (t_R and t_g) and baseline bandwidths (W_y and W_y'). See text for details.

The quantity k' is measured from the band maximum. For large samples, w_{xn} will also be large, and under these conditions eqns. 5–7a yield (approximately)

$$w_s = (4p\ w_x)/[1 - (k'/k_0)]^2 \tag{8}$$

Experimental values of w_s from ref. 18 (summarized in refs. 13 and 15) correlate well with eqn. 8, yielding an average value of $p = 0.8 \pm 0.2$ (1 S.D.). This is reasonably close to the expected value, $p = 5/8$.

Bandwidth vs. solute mass in gradient elution

For the case of two solutes X and Y that are separated under conditions of mass-overloaded HPLC, it has been shown that the resulting resolution will be the same in "corresponding" isocratic and gradient separations[17]. "Corresponding" systems in this case mean that values of the parameter b are approximately equal for X and Y in the gradient separation, and the average (isocratic) value of k_0 for compounds X and Y equals $(1/1.15b)$ in the gradient run. This situation is illustrated schematically in Fig. 2 for a sample size such that the two bands just touch in each separation (equal resolution). The baseline bandwidths, W_y (isocratic) and $W_{y'}$ (gradient) for compound Y, are defined in Fig. 2, as are the retention times (small sample, see ref. 16) for bands X and Y in isocratic (t_{Rx}, t_{Ry}) or gradient (t_{gx}, t_{gy}) elution.

From Fig. 2 we obtain the following relationships:

$$W_y = t_{Ry} - t_{Rx} \tag{9}$$

and

$$W_{y'} = t_{gy} - t_{gx} \tag{10}$$

The final bandwidth W (either isocratic or gradient) is the sum of contributions from (a) dispersion within the column (for a small sample) W_0, and (b) mass-overload of the column W_{th}[21]:

$$W^2 = W_0^2 + W_{th}^2 \tag{11}$$

W_0 for isocratic HPLC is given by

$$W_0 = \frac{1}{4}\, t_{Ry}\, N_0^{-1/2} \tag{12}$$

The quantity W_{th} can be derived as follows. W_{th} is the bandwidth that would be observed for a very large sample, where $W \approx W_{th}$. This is equivalent to assuming that $w_{xn} \gg 1$ in eqn. 5, which leads to

$$\begin{aligned} W_{th} &= \{(4p)\ [k_0/(1 + k_0)]^2\ (w_y/w_s)\}^{1/2}\ t_{Ry} \\ &= Z\ t_{Ry} \end{aligned} \tag{13}$$

Here, k_0 refers to the value for compound Y. Eqns. 9 and 11 (assuming w_{xn} large) then give

$$t_{Rx} = (1 - Z)\, t_{Ry} \tag{14}$$

Since values of t_R are given as $t_0(1 + k_0)$, eqn. 14 can be written as

$$k_x = k_y - (1 + k_y)\, Z \tag{15}$$

and from the definition of Z (eqn. 13)

$$k_x/k_y = 1 - [4p(w_y/w_s)]^{1/2} \tag{16}$$

Gradient retention t_g for a small sample is given[11] as

$$t_g = (t_0/b) \log(2.3\, k_{0g}\, b) + t_0 + t_D \tag{17}$$

when the value of k' at the beginning of the gradient (k_{0g}) is large (so-called "gradient" conditions). Here, t_D refers to the gradient dwell time. Eqn. 17 can be written for band X or Y to give t_g (t_{gx} or t_{gy}) as a function of k_{0g} for each compound: $(k_{0g})_x$ and $(k_{0g})_y$. These values of t_g (from eqn. 17) can then be combined to yield

$$t_{gy} - t_{gx} = (t_0/b) \log[(k_{0g})_y/(k_{0g})_x] \tag{18}$$

If we assume equal b values for each band (implying equal values of $S = \mathrm{d}(\log k')/\mathrm{d}\,\varphi$; see ref. 11), it can be shown[17] that the gradient parameters k_{0g} and isocratic parameters k_x and k_y are related as

$$(k_{0g})_y/(k_{0g})_x = k_y/k_x. \tag{19}$$

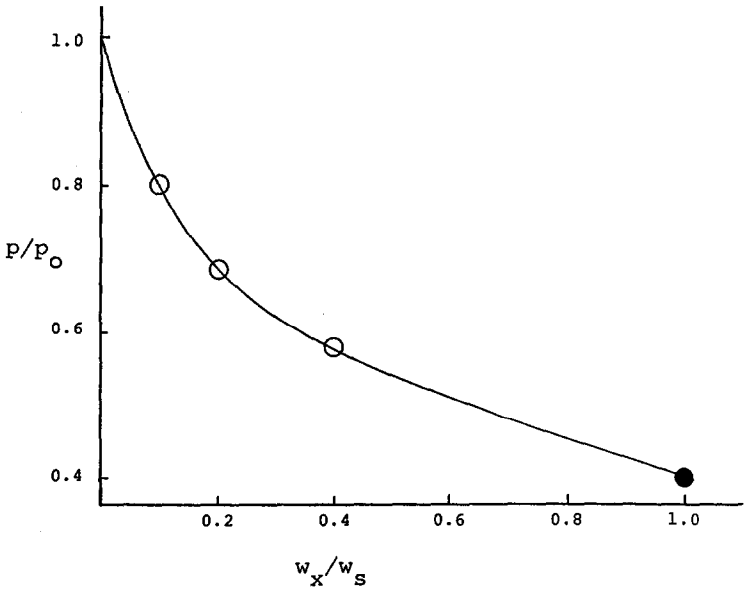

Fig. 3. Failure of the two-term Langmuir equation for larger sample sizes. Values of p/p_0 from Craig simulations with $n_c = 200$ and $k_0 = 1$.

Eqns. 10 ($W_y = W_{th}$), 16, 18 and 19 give finally

$$W_{th} = t_{gy} - t_{gx} = -(t_0/b) \log\{1 - [4p(w_y/w_s)]^{1/2}\} \quad (20)$$

Eqns. 11 (W_y replaces W) plus 20 provide a quantitative description of bandwidth in gradient elution as a function of experimental conditions.

Value of p for large values of w_x/w_s

We have noted[16] that eqn. 5 is accurate only for moderate overloading of the column ($w_x/w_s < 0.10$), *i.e.* eqn. 5 assumes that a Langmuir isotherm can be approximated by the first two terms of a polynomial expansion[21]. For larger values of w_x/w_s, values of N are larger than predicted by eqn. 5, corresponding to smaller values of the parameter p. If we let p_0 refer to the value of p in the absence of higher-order terms (*e.g.*, for small values of w_x/w_s), the ratio (p/p_0) then represents the magnitude of this effect (error in eqn. 5 due to the two-term Langmuir approximation). This is further illustrated in Fig. 3 for data (○) from Craig simulations of isocratic elution at large values of w_x/w_s; (p/p_0) is plotted *vs.* w_x/w_s*. This relationship (solid curve in Fig. 3) can be represented adequately by the empirical equation

$$p/p_0 = 1 - 0.6(w_x/w_s)^{0.43} \quad (21)$$

Eqn. 21 is useful for defining the range of w_x/w_s values for which eqns. 5, 8 and 20 are accurate, *i.e.* where $p/p_0 \approx 1$. Eqn. 21 can also be used (approximately) for correcting these relationships when $w_x/w_s \ll 1$.

Measurement of column saturation-capacity w_s

The effective use of preparative HPLC requires an initial estimate of the column capacity w_s. This can be determined as described in ref. 17 from the change in retention (t_g) with sample mass for an individual band X. There, the change in t_g which results from a large sample-mass w_x *vs.* a small sample of X was derived:

$$\Delta t_g = (t_0/b) \log(k'/k_0) \quad (22)$$

Here (k'/k_0) refers to retention values for a corresponding isocratic separation. Combining eqns. 8 an 22 then gives

$$w_s = (4p\ w_x)/[1 - 10^{-(b/t_0)\Delta t_g}]^2 \quad (23)$$

Alternatively, we can derive an expression for w_s from the bandwidth W_y (gradient elution) for a sample-mass w_x *vs.* the bandwidth W_0 for a small sample of X. Eqn. 11 first allows us to calculate W_{th} from values of W_y and W_0; rearrangement of eqn. 20 then yields

$$w_s = (4p\ w_x)/[1 - 10^{-(b/t_0)W_{th}}]^3 \quad (24)$$

* The dark circle in Fig. 3 for $w_x/w_s = 1$ is inferred from a preceding isocratic relationship, eqn. 17 of ref. 16, taking into account the 2.4-fold difference in p values (Craig *vs.* experimental).

Eqns. 23 and 24 are essentially the same relationship. In eqn. 23 the bandwidth is approximated by Δt_g, whereas in eqn. 24 the bandwidth is measured directly. For large values of w_x and/or N_0, Δt_g approaches W_{th}, and the two equations become equivalent.

Blockage effects

For sufficiently large samples (*e.g.*, $W_x/w_s > 0.05$), it is found that adjacent bands X and Y affect the elution of each other ("mixed-isotherm" effects[14,15]). The major result is earlier elution and a narrowing of the less-retained band X. Similar effects are observed in gradient elution[17]. This phenomenon, which we term "blockage", can be quantitatively described by means of a simple model. It is assumed that the second compound Y competes with X for sorption onto the initial part of the column, during the migration of X through the column. The magnitude of this effect can be quantitatively described in terms of a shortening (or blockage) of the column by a factor x, so far as the elution of X is concerned. Band X then moves through the shortened column more quickly, with less band broadening.

Blockage is expected to be more important in the gradient separation of peptides and proteins, because (for various reasons) larger samples can be conveniently injected. We therefore need to know how blockage affects gradient elution separation in a mass-overload mode. The (equivalent) fractional shortening x of the column (for elution of band X) as a result of the presence of band Y is described by

$$x = f_{yx}\,(w_x/w_s) \tag{25}$$

The empirical blockage-factor, f_{yx} is a function of the ratio of isocratic k_0 values (k_y and k_x) for Y and X:

$$f_{yx} = 2.25\,[(k_y/k_x) - 1]^{-0.33} \tag{26}$$

or, for $k_y/k_x > 10$

$$f_{yx} = 1 \tag{26a}$$

The displacement of band X as a result of blockage is illustrated in the hypothetical (mass-overloaded) example of Fig. 4 (gradient elution). The two bands would just touch if there were no interaction (blockage) between them, as shown by the separate injection of X (Fig. 4a) and Y (Fig. 4b). After injection of the mixture (Fig. 4c), however, blockage of the column by Y results in the displacement of the tail of X by the time Δt. This displacement Δt in turn determines the effect of blockage on separation.

In the case of isocratic separation, we can predict that Δt will be given by

$$\Delta t = x\,k_0\,t_0 \qquad \text{(isocratic)} \tag{27}$$

This is tested in Table I for the isocratic separation of hydroxyethyltheophylline (HET) and 7-β-hydroxypropyltheophylline (HPT), reported in ref. 15. Good agreement is found between experimental values of Δt and values from eqn. 27.

The extension of eqn. 27 to gradient elution suggests that the band displacement Δt will be equivalent to that in isocratic elution, if there is a corresponding change in

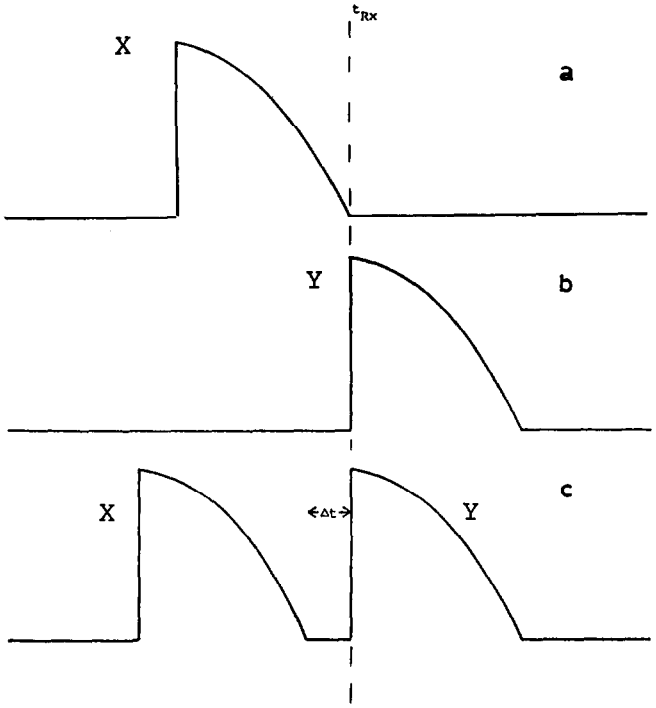

Fig. 4. Illustration of the effect of "blockage" on mass-overloaded separations by gradient elution. See text.

k_{0g} for the gradient separation by a factor $(1 - x)$. The predicted change in t_{gx} (see Fig. 2) is then (eqn. 17)

$$\Delta t = (t_0/b) \log(1 - x) \qquad \text{(gradient)} \tag{28}$$

The importance of blockage in a gradient separation can be inferred by comparing Δt (eqn. 28) with W_y (eqns. 11 and 20). When Δt is small compared to W_y, blockage can be ignored. Alternatively, when Δt is not small compared to W_y, it is important to correct predictions of separation (resolution) by means of eqn. 28.

TABLE I

QUANTITATIVE PREDICTION OF BAND DISPLACEMENT Δt DUE TO "BLOCKAGE"

Value of Δt for HET (X) as a result of blockage by HPT (Y). Data from ref. 15; see text for details.

w_x (mg)	(w_x/w_s)	*Band displacement* Δt	
		Experimental	*Calculated**
2.5	0.0104	0.10	0.07
10	0.042	0.33	0.28
25	0.104	0.70	0.70

* Eqn. 27; variation of p/p_0 accounted for in derivation of eqns. 25 and 26.

Effect of k_{0g} on mass-overloaded elution bands: limits on bandwidth in gradient elution

If sample size is increased indefinitely in isocratic elution, the solute band will continue to increase in width until the band front runs into t_0, *i.e.* when w_x approaches w_s. This is illustrated in Fig. 5a for some representative Craig simulations (isocratic elution, varying sample size). If the sample size is likewise increased in gradient elution, the band widens up to a certain point (as w_x approaches w_s), but no further. In this case the band may not run into t_0. This is illustrated in Fig. 5c for corresponding mass-overloaded separations by gradient elution ($k_{0g} = 1000$). That is, under gradient conditions such that k_0 is large, there is no bleed of sample from the column —as long as $w_x < w_s$. We also see (Fig. 5c) that there is no elution before a time $t/t_0 = 3$, corresponding to a (small sample) k' of 100 at this point in the gradient.

If gradient conditions are changed so as to vary k_{0g} (*e.g.*, change the starting concentration of organic solvent in the mobile phase), here will generally be little effect on the elution band as long as $k_{0g} > 100$. The band will simply be displaced in the chromatogram by a distance corresponding to the difference in small-sample t_g values. This is illustrated in Fig. 5b for the same separations as in Fig. 5c, except for $k_{0g} = 100$ (instead of 1000).

As a practical consequence of the behavior illustrated in Fig. 5, gradient bands will usually broaden up to the point where $w_x = w_s$, and then stay the same size for further increase in w_x. The sample mass in excess of w_s will then be eluted at t_0. This can confuse the measurement of w_s by means of eqn. 20, if column bleed (when $w_x > w_s$) is overlooked.

EXPERIMENTAL

No new experimental data are reported in this paper. Computer simulations were carried out on an IBM-XT personal computer. Bandwidths reported here are usually "cumulative" values, measured as in ref. 12. Retention times are variously peak-maximum values or cumulative values, and are specified when discussed.

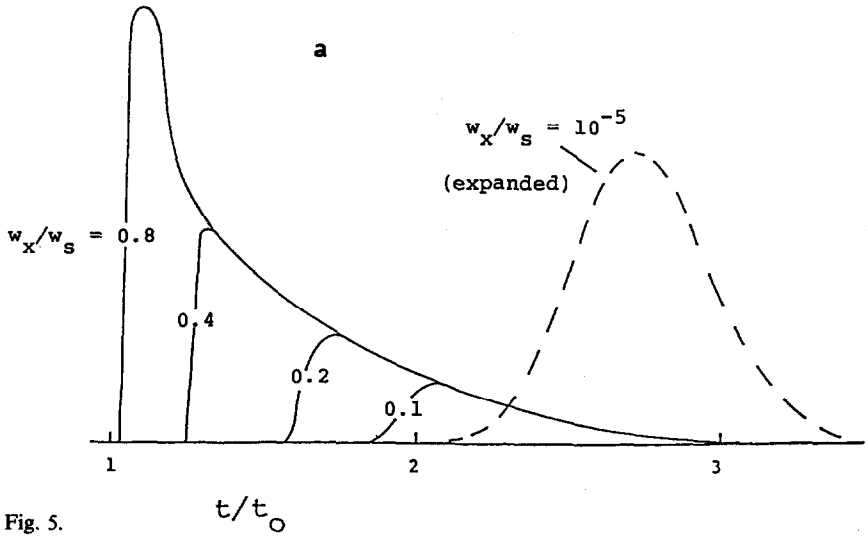

Fig. 5.

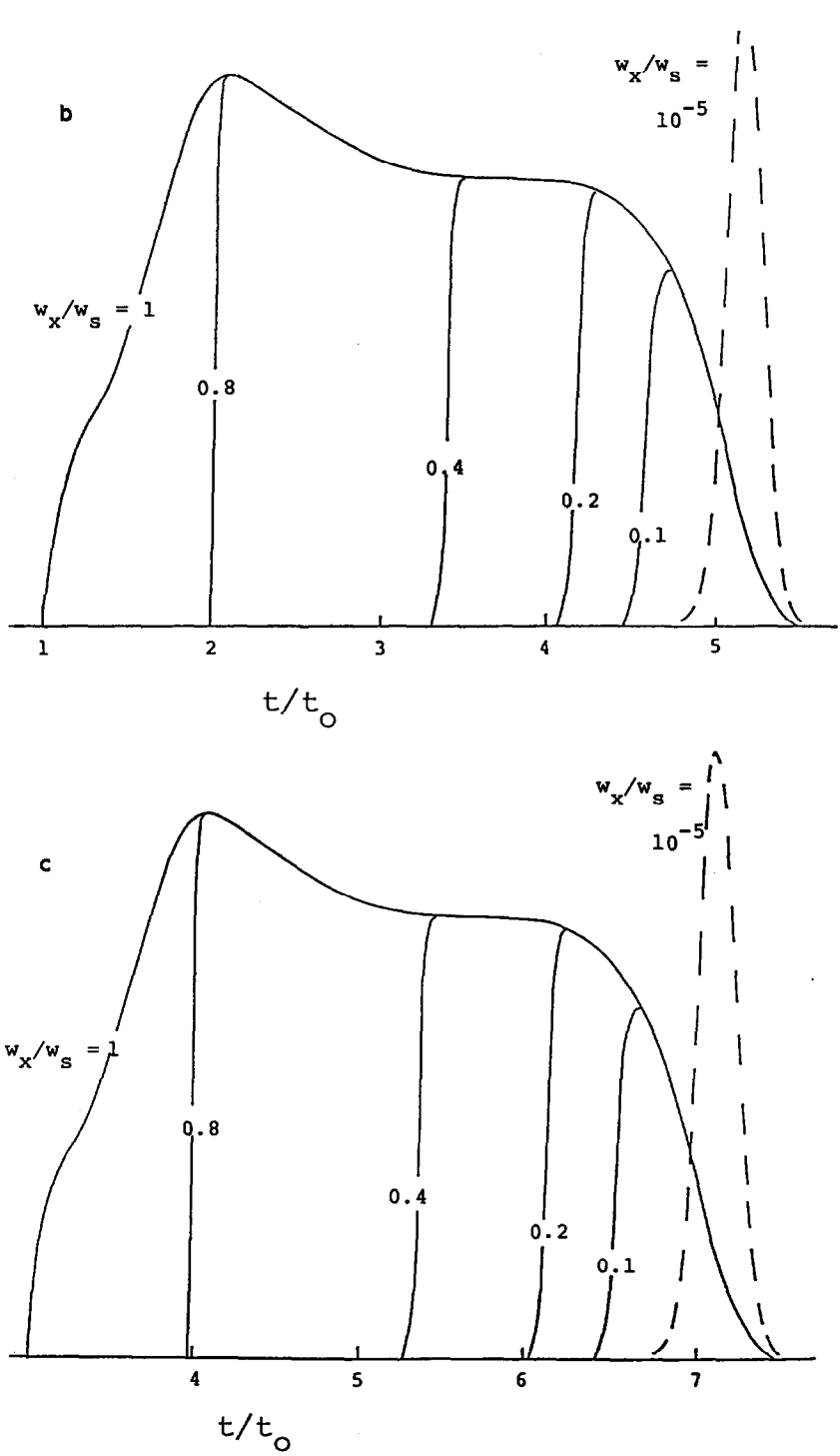

Fig. 5. Mass-overload compared in isocratic *vs.* gradient elution, and for different values of k_{0g}. Craig simulations, n_c = 100; (a) isocratic separation, k_0 = 1.75; (b) gradient elution, k_{0g} = 100, b = 0.5; (c) gradient elution, k_{0g} = 1000, b = 0.5.

RESULTS AND DISCUSSION

Craig simulations were carried out as described in Theory for a broad range of separation conditions (varying values of k_{0g}, b, w_x/w_s and n_c). Data for small samples ($w_x/w_s = 10^{-5}$) were first compared with corresponding results from rigorous theory (which is applicable in this case[20], but not for large samples), as a means of verifying the accuracy and applicability of these Craig simulations. Then, additional comparisons were made of Craig-simulated bandwidths *vs.* values calculated by means of eqn. 20, as a means of (a) further verifying the utility of Craig simulation for large samples, and (b) confirming the scope and accuracy of eqn. 20. Finally, some additional questions concerning gradient elution under mass-overload conditions were examined by means of Craig simulations.

Verification of Craig simulations for small samples

For the case of a small sample (no mass overload), retention time in gradient elution is given[11] as

$$t_g = (t_0/b) \log[(2.3k_{0g}b) + 1] + t_0 + t_D \tag{29}$$

In the case of Craig simulations, we can assume $t_D = 0$. Likewise, baseline bandwidth W_0 (or W_y) is given[11] as

$$W_0 = 4G\, t_0 \{1 + [k_{0g}/(2.3k_{0g}b + 1)]\}\, N_0^{-1/2} \tag{30}$$

TABLE II

COMPARISON OF GRADIENT ELUTION RETENTION (t_g) AND BANDWIDTH ($W = W_0$) FOR A SMALL SAMPLE ($w_x/w_s = 10^{-5}$): CRAIG SIMULATIONS *VS.* EXPLICIT CALCULATIONS

k_{0g}	n_c	b	t_g/t_0*		W/t_0	
			Craig	*Eqn. 29*	*Craig*	*Eqn. 30*
10	20	0.05	3.21	3.19	0.932	0.938
	50		3.20	3.19	0.586	0.602
	100		3.20	3.19	0.414	0.428
	200		3.20	3.19	0.293	0.303
100	10	0.5	5.17	5.13	1.38	1.34
	20		5.15	5.13	0.974	0.970
	50		5.14	5.13	0.614	0.622
	100		5.13	5.13	0.434	0.440
100	50	0.1	14.79	14.80	2.50	2.57
		0.2	9.36	9.36	1.34	1.35
		1.0	3.38	3.36	0.360	0.374
		2.0	2.34	2.33	0.224	0.238
	Average error			±0.02%		±2%

* Cumulative values of t_g (50% elution of band, ref. 12).

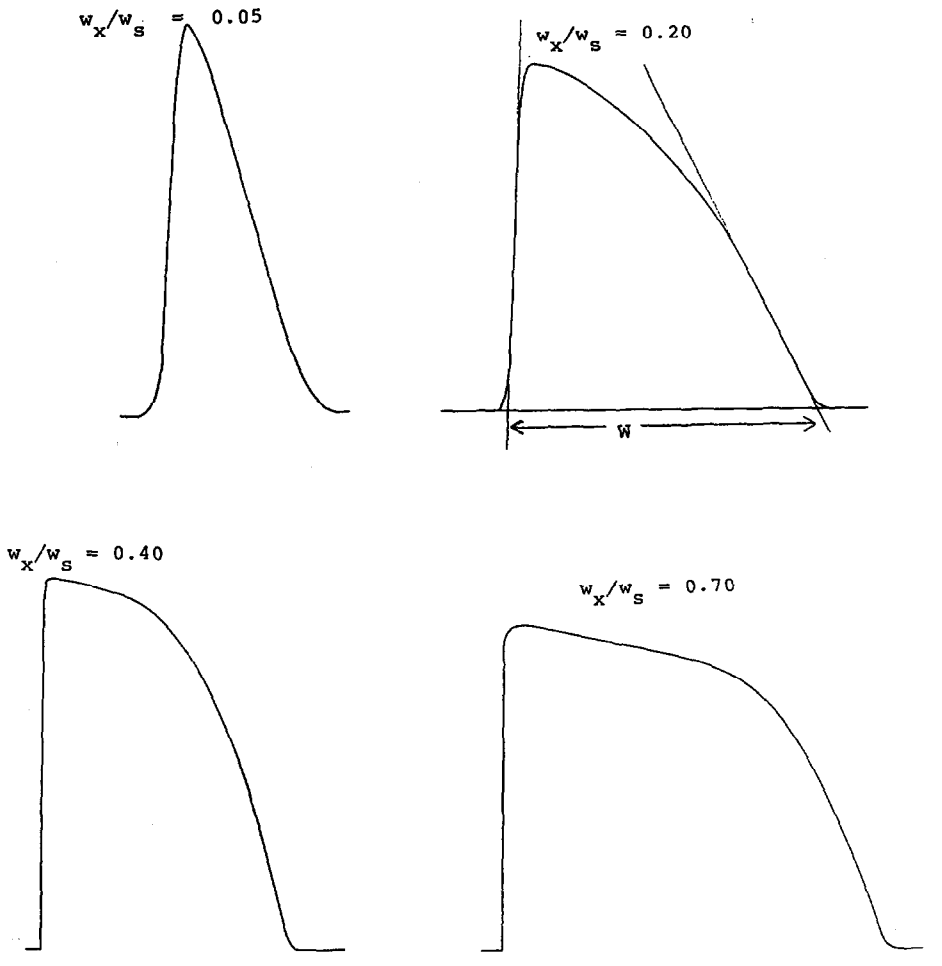

Fig. 6. Band shape in mass-overloaded gradient elution. Craig simulations; $n_c = 200$, $k_{0g} = 100$, $b = 0.50$. Values of w_x/w_s indicated in Figure. Similar band shapes observed for other values of b.

The quantity G is a gradient compression factor that can be calculated as a function of b[20]. Values of t_g and W_0, determined from eqns. 29 and 30, are compared in Table II with values determined from Craig simulations. Good agreement is seen for all cases examined, even for small values of n_c.

Characteristics of mass-overloaded sample bands in gradient elution

Band shape. In isocratic HPLC, mass-overloaded solute bands assume a characteristic "right-triangle" appearance, as illustrated in Fig. 2 and discussed in refs. 16 and 21. As sample size is increased in gradient elution, the resulting bands eventually resemble a rounded right-triangle or "shark fin"[17]. However, many extraneous factors can affect band shape, apart from the separation *per se*. For this reason it is interesting to examine band shape in gradient elution as sample size is

increased, by means of Craig simulations (which are not subject to these extraneous effects).

Fig. 6 illustrates typical band shapes for mass-overloaded gradient elution, as obtained from Craig simulations. For small samples (*e.g.*, $w_x/w_s \ll 0.01$), the bands are near-Gaussian with a tendency to slight fronting (due to the gradient). Moderate overloading of the column results in bands with a right-triangle appearance, much as in isocratic elution (*e.g.*, for $w_x/w_s = 0.05$ in Fig. 6). Further increase in sample size (*e.g.*, for $w_x/w_s = 0.20$ or 0.40) gives rise to the "shark-fin" bands noted above. Still larger samples (*e.g.*, $w_x/w_s = 0.70$ in Fig. 6) lead to further band distortion with an extended sloping top, but practical HPLC separations seldom allow this degree of column overloading.

Similar bandshapes (as in Fig. 6) result for other values of N_0, as long as the ratio ($N_0\ w_x/w_s$) is the same, *e.g.*, multiplying N_0 by 4 for the separations in Fig. 6 should result in the new band for $w_x/w_s = 0.05$ resembling the old band (Fig. 6) for $w_x/w_s = 0.20$.

The rounding of the elution band relative to isocratic separation is mainly due to "gradient compression" during elution of the band from the end of the column. That is, the shape of the band on the column is more nearly that of a right triangle, but during elution the band-tail is accelerated (and rounded) by the gradient. This is illustrated in Fig. 7 for sample bands just before (– – –) and after they leave the column (——), in both (a) isocratic and (b) gradient elution. The corresponding bands in Fig. 7 have been superimposed for a better comparison of their shapes immediately before and after elution. This example is typical for intermediate sample sizes ($0.05 < w_x/w_s < 0.40$).

Measurement of bandwidth. Bandwidth W in mass-overloaded gradient elution is conveniently measured as shown in Fig. 6 (for $w_x/w_s = 0.20$). For larger plate numbers ($N_0 > 200$), the extrapolated tail of the band is approximately equal to the retention time t_g for a small sample, similar to the case for mass-overloaded isocratic separation (see example of Fig. 2). This was true ($\pm 0.1\ t_0$), for example, in the case of Craig simulations with $n_c = 200$, $k_{0g} = 100$, $b = 0.5$, and w_x/w_s varied from 0.05 to 0.40. This observation can in some cases simplify the measurement of bandwidth in mass-overloaded separations, *e.g.*, when two bands severely overlap. In the present study, values of W are reported on a 4-σ basis* (see ref. 12), in order to insure comparability with our earlier studies of mass-overloaded isocratic elution by means of Craig simulations. Comparison of these (4σ) values of W with values determined as in Fig. 5 shows agreement within $\pm 5\%$, except for (w_x/w_s) > 0.40.

Bandwidth in mass-overloaded gradient elution

Craig simulations. Simulations of bandwidth W *vs.* sample size w_x were carried out for different conditions (varying n_c, k_{0g}, b and w_x/w_s). Values of W_{th} should be independent of N_0 and n_c, but this is only true for adequately large values of n_c. As an example for one set of conditions ($k_{0g} = 100$, $b = 0.50$, $w_x/w_s = 0.05$), the following values of W_{th} *vs.* n_c were found: $n_c = 20$, 50, 100, 200, 400; $W_{th}/t_0 = 0.33$, 0.35, 0.38, 0.41, 0.42. For $n_c > 100$, values of W_{th} are constant within $\pm 5\%$.

* That is, 2-σ bandwidths were determined as in ref. 12 (16–84% cumulative elution) and then multiplied by 2.

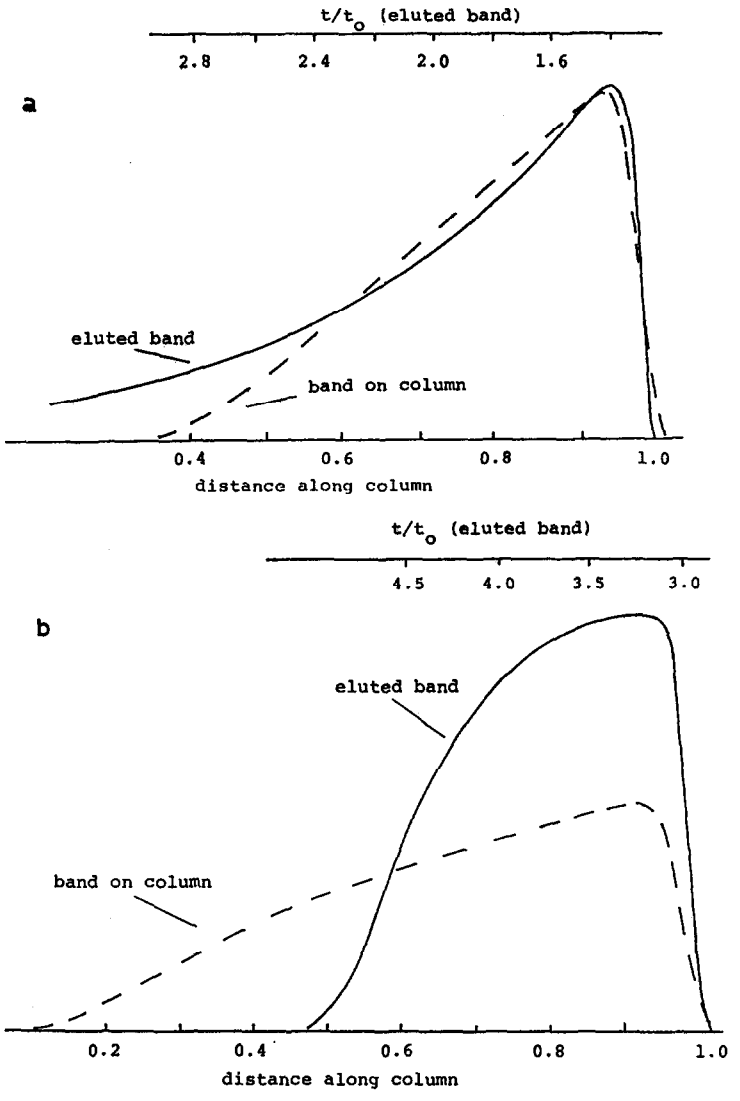

Fig. 7. Comparison of band shape on the column (just before elution) with the elution band for mass-overloaded separation. Craig simulations with $n_c = 50$, $w_x/w_s = 0.40$; (a) isocratic separation, $k_0 = 1$; (b) gradient separation, $k_{0g} = 100$, $b = 0.5$.

Values of W were first obtained from these Craig simulations, then eqn. 11 was used to derive values of W_{th}. Fig. 8 shows three sets of W_{th} values (different values of b) as a function of sample size w_x/w_s. It is seen that these data points for a given value of b fall on a straight line when plotted on a log–log basis as in Fig. 8 (values of W_{th} do not vary with change in k_0, as expected when k_{0g} is large). An empirical equation describes these data with an average error of less than $\pm 5\%$ in W:

$$W_{th} = 2.3\ (t_0/b)\ (w_x/w_s)^{0.85} \tag{31}$$

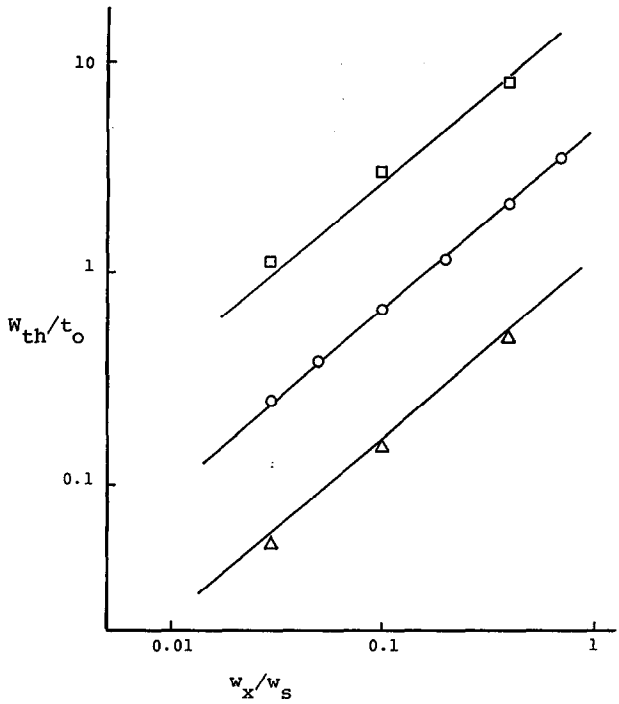

Fig. 8. Dependence of mass-overload contribution to bandwidth (W_{th}) on sample size w_x/w_s. Craig simulations, $n_c = 200$, $k_{0g} = 100$, $b = 0.125$ (□), 0.50 (○), and 2 (△). Solid lines are calculated from eqn. 31.

Eqn. 31 should prove useful in predicting separation in mass-overloaded gradient elution because of its simplicity. Experimental values of W_{th} will be 1.5-fold larger than predicted by eqn. 31 (for Craig simulation), because of the 2.4-fold larger value of p in experimental systems *vs.* Craig simulations. However this error cancels, if values of w_s are measured via eqn. 24.

Table III compares Craig-simulation values of W (corresponding to the data of Fig. 8) with values calculated from eqns. 11 and 20. Good agreement is observed.

Experimental bandwidths from ref. 17. Eqn. 20 can be applied to experimental data reported in ref. 17 for the mass-overloaded elution of HPT by gradient elution. For experimental systems, $p_0 = 1.5$ rather than 5/8 for Craig simulation. The conditions for these runs were as follows: $b = 0.35$, $t_0 = 1.43$ min, k_0 (isocratic) = 3.15 and $N_0 = 5750$. The resulting value of W_0 (eqn. 30) is 0.186 min. Sample size was varied from 1.0 to 25 mg for a column whose w_s value was determined (isocratic measurements[17]) to be 240 mg. Eqns. 11 and 20 then allowed the prediction of bandwidths W_y as a function of sample mass w_x. These results are summarized in Table IV, with satisfactory agreement between predicted and experimental bandwidth values.

Bandwidth as a function of column plate-number and sample size. This has been discussed in detail in refs. 16 and 21 for isocratic separation. The column plate number N_0 affects only W_0 in eqn. 11, meaning that for larger samples the value of N_0 becomes less important. This is illustrated in Fig. 9 for Craig simulations based on different

TABLE III

CRAIG-SIMULATION VALUES OF BANDWIDTH W IN GRADIENT ELUTION: COMPARISON WITH VALUES FROM EQNS. 11 AND 20

Conditions: $n_c = 100$, $k_{0_s} = 100$, p/p_0 from Fig. 3.

w_x/w_s	W/t_0					
	$b = 0.50$		$b = 0.125$		$b = 2$	
	Craig	*Calculated*	*Craig*	*Calculated*	*Craig*	*Calculated*
10^{-5}	0.43	0.43	1.45	1.45	0.158	0.158
0.03	0.50	0.50	1.83	1.77	0.166	0.170
0.05	0.58	0.56				
0.10	0.80	0.72*	3.34	2.71*	0.220	0.213*
0.20	1.25	1.13*				
0.40	2.18	2.56*	8.28	10.2*	0.51	0.65*
0.70	3.60	(2.2+)**				

* Corrected for difference between Craig simulations and eqn. 5 (dashed *vs.* solid curves of Fig. 1).
** Indeterminate value.

values of N_0. For example, if $w_x/w_s > 0.05$, there is no advantage to an N_0-value greater than 500, *i.e.* the same separation (same bandwidths) will result.

Column saturation capacity w_s

The saturation capacity of the column is the main factor that determines maximum sample size. A knowledge of the value of w_s is therefore important for designing efficient preparative-scale separations. Eqns. 23 and 24 furnish a basis for estimating values of w_s from two gradient runs, one with a small sample and one with a value of w_x sufficient to result in appreciable band broadening due to mass overload. We will now examine the use of these two relationships for measuring w_s, using Craig simulations to illustrate their use and examine their reliability.

TABLE IV

COMPARISON OF EXPERIMENTAL BANDWIDTHS WITH VALUES PREDICTED BY EQNS. 11, 20 AND 22

Data for HPT as a function of sample size in reversed-phase gradient elution[17]; see text for details.

w_x *(mg)*	w_x/w_s	p/p_0*	W_y *(min)*	
			Experimental	*Calculated***
1.0	0.004	0.94	0.37	0.35
2.5	0.010	0.92	0.55	0.52
10	0.042	0.85	1.13	1.11
25	0.104	0.77	2.07	2.10

* From Fig. 3.
** Eqns. 11 and 20 with $p_0 = 1.5$; *e.g.*, $p = 0.94 \cdot 1.5$ for $w_x = 1$ mg.

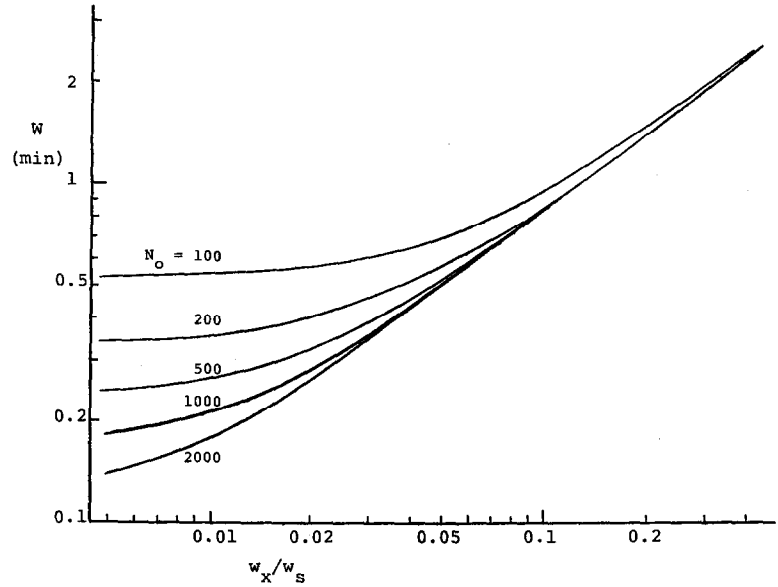

Fig. 9. Dependence of bandwidth W on sample sze w_x/w_s and plate number N_0 (for a small sample). Calculations based on eqns. 11 and 31 (derived from Craig simulations).

The sample size w_x used in the mass-overloaded gradient run must be large enough to achieve a significant increase in bandwidth or decrease in retention time t_g. If a change in retention time is used to estimate w_s (eqn. 23), it is also necessary that the column plate number N_0 be large enough so that the shape of the elution band closely approaches a "shark-fin" as in Fig. 2. That is, eqn. 23 assumes that bandwidth can be approximated by Δt_g. Consider the following example based on Craig simulations for $n_c = 100, k_{0g} = 100$ and $b = 0.50$ ($p = 5/8$). A w_s value of 100 mg was assumed, and for sample-sizes w_x of 10^{-5} and 5 mg the following results were obtained: (10^{-5} mg), $W = W_0 = 0.434\, t_0$, $t_g = 5.13\, t_0$; (5 mg), $W = 0.58\, t_0$, $t_g = 5.00\, t_0$. A value of W_{th} from eqn. 11 was obtained first: $W_{th} = 0.25\, t_0$. Eqn. 24 was next used with this value to estimate w_s, assuming $p = p_0$: $w_s = 120$ mg. A value of $w_x/w_s = 0.025$ was then calculated, based on this initial estimate of w_s. The latter value of w_x/w_s was used with eqn. 21 to estimate $p/p_0 = 0.88$, and $p = 0.55$. Recalculation of w_s with this new value of p (eqn. 21) gave $w_s = 106$ mg. This, in turn, was used to generate new values of w_x/w_s and p, giving a final value of $w_s = 104$ mg. This result from successive approximations is reasonably close to the actual value (100 mg) used in the original Craig simulations that generated the starting data for this example. Repetition of these calculations for w_x values of 10, 20 and 40 mg gave w_s values of 86–119 mg (after correction for the failure of eqn. 5 shown in Fig. 2 —dashed *vs.* solid curves).

The similar use of eqn. 23 (instead of eqn. 24) with the change in t_g for a 3-mg sample gave $w_s = 382$ mg (an error of 282%!). The reason for this is that the low plate number for this run ($N_0 = 160$) resulted in a considerable rounding of the elution band, with only a poor resemblance to a "shark-fin". This illustrates one limitation in the use of eqn. 23 and suggests that eqn. 24 may be better suited for estimating w_s values.

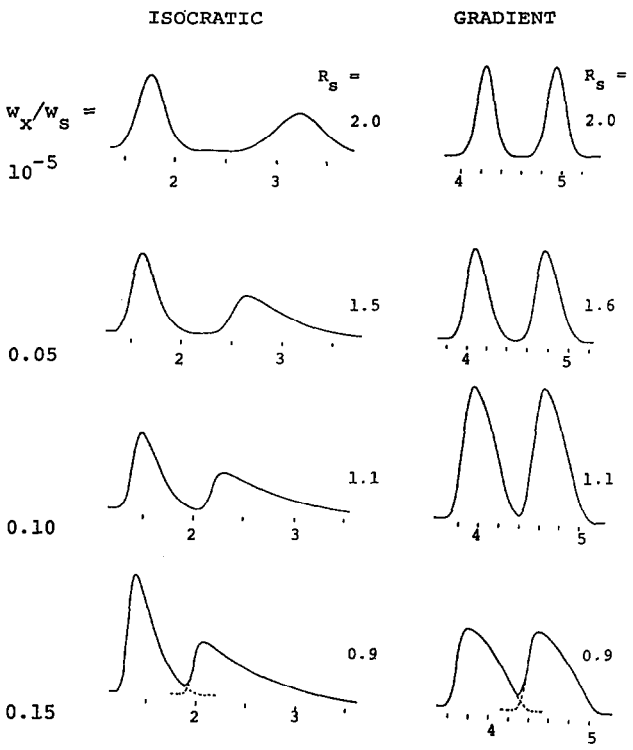

Fig. 10. Resolution in "corresponding" isocratic and gradient systems as a function of sample size w_x/w_s. Craig simulations; isocratic conditions: n_c = 76 (X), 123 (Y), (N_0 = 180); k_0 = 0.74 (X) and 2.22 (Y); gradient conditions: n_c = 100 (N_0 = 180); b = 0.68 (X and Y); k_{0g} = 100 (X) and 300 (Y).

Resolution in isocratic vs. gradient elution

Earlier, we showed[17] for "corresponding" isocratic and gradient systems that the resolution of any two bands in the chromatogram should be the same when sample sizes are equal in each run. This demonstration was based both on theoretical arguments and experimental examples. Fig. 10 provides a further confirmation of this conclusion, based on Craig simulations. Conditions for the isocratic runs are: N_0 = 180 and k_0 equal 0.74 and 2.22 for compounds X and Y, with sample size w_x/w_s varied as shown in Fig. 10. The corresponding gradient runs have an average value of k' (small sample) equal to the geometric mean of the isocratic k_0 values: $\bar{k}$ = 1.28 and b = (1/1.15 $\bar{k}$) = 0.68, with N_0 = 180. Values of k_{0g} for the gradient runs were selected equal to 100 and 300 for X and Y (note eqn. 19); the separation factor α is equal to 3.0 for both the isocratic and gradient runs.

Comparing the various isocratic and gradient simulations of Fig. 10, we see that equivalent resolution is obtained when the sample size is the same —as predicted for "corresponding" separations[17]. Values of resolution R_s in Fig. 10 are calculated from bandwidths at half-height:

$$R_s = 1.18\,(t_2 - t_1)/(W_1 + W_2) \qquad (32)$$

Here t_1 and t_2 are the measured retention times for the first and second bands, and W_1 and W_2 are the bandwidths of each band, measured at half-height. Eqn. 32 is more convenient to use than the usual equation of R_s based on the measurement of baseline bandwidths, particularly for preparative separations.

CONCLUSIONS

Craig simulations of mass-overloaded gradient elution HPLC were carried out in order to better define the relationship between separation, sample size and experimental conditions. A similar approach, used previously for isocratic elution[12,14], resulted in useful comparisons between Craig simulations and actual experimental systems[13,15]. Results from gradient-elution Craig simulations carried out in this study are in general agreement with theory derived here and elsewhere[17]; this supports the validity of both the Craig simulations and our present theory for these separations. A limited set of experimental data reported previously (small molecules, ref. 17) also agrees with the equations derived here.

Resolution and bandwidth can be predicted quantitatively as a function of sample size and different experimental conditions, using any of three different relationships derived here. As noted earlier[13,15,16], bandwidths from Craig simulations are generally smaller than corresponding experimental bandwidths—for reasons that are still not clear. The Knox-Pyper treatment of mass-overloaded isocratic HPLC[21] and our adaptation of that model[16] is limited to relatively small samples, because of the use of a 2-term approximation to the Langmuir isotherm. In this paper we have examined these complications and reconciled them in terms of an empirical factor p. The use of this empirical factor allows semi-quantitative predictions of bandwidth in mass-overloaded isocratic or gradient elution for any sample size. We have also extended the present treatment to include mixed-isotherm effects ("blockage") that are involved in the gradient elution separation of any multi-component sample.

In the design of preparative separations, it is important to be able to estimate the column saturation-capacity w_s. Here we describe a simple procedure for determining w_s from only two experimental gradient-elution runs. The use of changes in bandwidth as sample size is varied seems to be the preferred approach.

We believe that the present study provides a basis for a better understanding of the preparative separation of any sample by gradient elution. The Craig-simulation model has also been established as a useful tool for exploring questions that are too complex to model analytically. Subsequent papers will illustrate this potential in the study of various aspects of the preparative separation of protein samples by means of gradient elution.

GLOSSARY OF SYMBOLS

b	gradient steepness parameter, equal to $V_m \Delta\varphi S/t_G F$
C, C', C''	empirical constants defined in eqns. 4, 9 and 10 of ref. 23
C_x	concentration of solute in mobile phase (mg/l)
f_{yx}	"blockage" factor; see eqn. 27
F	mobile phase flow-rate (ml/min)

G	gradient compression factor[20]
$\bar{k}$	effective or average value of capacity factor k' during gradient elution (for a small sample)
k'	capacity factor of a solute band; here k' is used to denote the k' value for a mass-overloaded band, in distinction to k_0 for the band when the sample size is small
k_i	capacity factor k_0 of the solute at the column inlet at some time during gradient elution (eqn. 4)
k_0	isocratic capacity factor k' for a small sample
k_{01}, k_{02}	values of k_0 for two different sites 1 and 2; eqn. 2 of ref. 23
k_{0g}	value of k_0 for a solute at the beginning of the gradient
$(k_{0g})_x$, $(k_{0g})_y$	values of k_{0g} for solutes X and Y
k_x, k_y	values of k_0 for solutes X and Y (isocratic elution)
N	column plate number (eqn. 5)
N_0	value of N for a small sample
p	empirical factor that takes into account differences in band-broadening between experimental and Craig systems, as well as failure of 2-term Langmuir isotherm approximation for larger samples; for $w_x/w_s < 0.10$, $p = p_0$ is equal to 1.5 for experimental systems and 5/8 for Craig simulations (eqn. 21)
p_0	value of p for small values of w_x/w_s; equal to 5/8 for Craig simulations, 1.5 for experimental systems
R	fraction of total solute in the mobile phase (eqn. 3)
R_s	resolution of two adjacent bands; defined here by similar eqns. 34 (this paper) or 5 (ref. 5)
S	in isocratic reversed-phase HPLC, d (log k')/dφ
t_D	dwell time of HPLC system (min)
t_g	retention time (min) in gradient elution
t_{gx}, t_{gy}	value of t_g for solute X or Y (small sample)
t_G	gradient time (min)
t_0	column dead-time (min)
t_R	retention time (min) in isocratic elution
t_{Rx}, t_{Ry}	value of t_R for solutes X and Y (small sample)
V_m	column dead-volume (ml); equal to $F\,t_0$
w_s	column saturation capacity (mg); maximum amount of solute that can be held by the stationary phase
w_{s1}, w_{s2}	values of w_s for two different sites (1 and 2) in the stationary phase; see eqn. 2 of ref. 23
w_x	mass of sample X injected onto the column (mg)
w_{xn}	loading function, equal to $[k_0/(1 + k_0)]^2\, N_0\, (w_x/w_s)$
w_{xs}	mass of sample X in the stationary phase (mg)
W	bandwidth (min); defined as in Fig. 2 (for $w_x/w_s = 0.2$)
W_0	value of W for a small sample
W_{th}	contribution to W from mass overloading (eqn. 11)
W_y	value of W for solute Y in isocratic separation (Fig. 2)
$W_{y'}$	value of W for solute Y in gradient elution (Fig. 2)

x	equivalent reduction in column length because of "blockage" of the front of the column by a second band Y; band X (less retained) then is retained only by the fraction $(1 - x)$ of the column
X, Y	solutes X (less retained) and Y (more retained)
z	slope of plots of log W_{th} *vs.* log w_x; see ref. 23 (Figs. 5–11)
Z	function defined in eqn. 13
Δt	displacement of band X as a result of "blockage"; see Fig. 4
Δt_g	change in t_g as a result of column overload (eqn. 24)
φ	volume fraction of organic modifier in the mobile phase
$\Delta\varphi$	change in φ during the gradient
ψ	phase ratio, equal to the mass of stationary phase (mg) divided by the total mobile phase volume (ml) (in the column or a Craig stage)

APPENDIX I

Empirical function for calculating R as a function of k_0 and sample size

The function R is determined for each stage after each transfer by means of the following algorithm:

(1) if $w_x\, k_0 > 100$ then $R = (w_x - 1)/w_x$

(2) define $Q = w_x\,(2/w_x)^{-0.2}\, k_0$
if Q < 2 then $R = 0.23\, Q^{1.13}$

(3) if $2 < Q < 34$ then $R = 1 - 1.05\, Q^{-0.94}$

(4) if $Q > 34$ then $R = (w_x - 1)/w_x$

REFERENCES

1 J. Rivier, R. McClintock, R. Galyean and H. Anderson, *J. Chromatogr.*, 288 (1984) 303.
2 R. Sitrin, P. DePhillips, M. DiPaolo and J. Dingerdissen, *presented at the 3rd Washington Symposium on Preparative Scale Liquid Chromatography, Washington, DC, May 4–5, 1987.*
3 M. N. Schmuck, D. L. Gooding and K. M. Gooding, *J. Chromatogr.*, 359 (1986) 323.
4 M. A. Rounds, W. Kopaciewicz and F. E. Regnier, *J. Chromatogr.*, 362 (1986) 187.
5 Y. S. Kim, B. W. Sands and J. L. Bass, *J. Liq. Chromatogr.*, 10 (1987) 839.
6 T. Ueda and Y. Ishida, *J. Chromatogr.*, 386 (1987) 273.
7 W. Kopaciewicz, S. Fulton and S. Y. Lee, *J. Chromatogr.*, 409 (1987) 111.
8 F. E. Regnier and R. Stringham, *presented at the 3rd Washington Symposium on Preparative Scale Liquid Chromatography, Washington, DC, May 4–5, 1987.*
9 R. R. Janzen and K. K. Unger, *presented at the 3rd Washington Symposium on Preparative Scale Liquid Chromatography, Washington, DC, May 4–5, 1987.*
10 F. L. De Vos, D. M. Robertson and M. T. W. Hearn, *J. Chromatogr.*, 392 (1987) 17.
11 L. R. Snyder and M. A. Stadalius, in Cs. Horváth (Editor), *High-Performance Liquid Chromatography —Advances and Perspectives*, Vol. 4, Academic Press, New York, 1986, p. 195.
12 J. E. Eble, R. L. Grob, P. E. Antle and L. R. Snyder, *J. Chromatogr.*, 384 (1987) 25.
13 J. E. Eble, R. L. Grob, P. E. Antle and L. R. Snyder, *J. Chromatogr.*, 384 (1987) 45.
14 J. E. Eble, R. L. Grob, P. E. Antle and L. R. Snyder, *J. Chromatogr.*, 405 (1987) 1.
15 J. E. Eble, R. L. Grob, P. E. Antle, G. B. Cox and L. R. Snyder, *J. Chromatogr.*, 405 (1987) 31.
16 L. R. Snyder, G. B. Cox and P. E. Antle, *Chromatographia*, 24 (1987) 82.
17 J. E. Eble, R. L. Grob, P. E. Antle and L. R. Snyder, *J. Chromatogr.*, 405 (1987) 51.
18 B. L. Karger, L. R. Snyder and Cs. Horváth, *An Introduction to Separation Science*, Wiley-Interscience, New York, 1973, pp. 110–116.
19 J. J. Stranahan and S. N. Deming, *Anal. Chem.*, 54 (1982) 1540.
20 L. R. Snyder, in Cs. Horváth (Editor), *High-performance Liquid Chromatography —Advances and Perspectives*, Vol. 1, Academic Press, New York, 1980, p. 205.
21 J. H. Knox and H. M. Pyper, *J. Chromatogr.*, 363 (1986) 1.
22 H. Poppe and J. C. Kraak, *J. Chromatogr.*, 255 (1983) 395.
23 G. B. Cox, P. E. Antle and L. R. Snyder, *J. Chromatogr.*, 444 (1988) 325.